Wind and Structures, *Vol. 23, No. 4 (2016) 367-383*
DOI: http://dx.doi.org/10.12989/was.2016.23.4.367

Mathematical explanation on the POD applications for wind pressure fields with or without mean value components

Jun-Feng Zhang[*1], Yao-Jun Ge[2a], Lin Zhao[2b] and Huai Chen[1]

[1]*School of Civil Engineering, Zhengzhou University, Zhengzhou 450001, China*
[2]*State Key Laboratory for Disaster Reduction in Civil Engineering, Tongji University, Shanghai 200092, China*

(Received October 22, 2015, Revised July 14, 2016, Accepted August 21, 2016)

Abstract. The influence mechanism of mean value components, noted as $\mathbf{P}_0$, on POD applications for complete random fields $\mathbf{P}_C(t)$ and fluctuating random fields $\mathbf{P}_F(t)$ are illustrated mathematically. The critical philosophy of the illustration is introduction of a new matrix, defined as the correlation function matrix of $\mathbf{P}_0$, which connect the correlation function matrix of $\mathbf{P}_C(t)$ and $\mathbf{P}_F(t)$, and their POD results. Then, POD analyses for several different wind pressure fields were presented comparatively as validation. It's inevitable mathematically that the first eigenmode of $\mathbf{P}_C(t)$ resembles the distribution of $\mathbf{P}_0$ and the first eigenvalue of $\mathbf{P}_C(t)$ is close to the energy of $\mathbf{P}_0$, due to similarity of the correlation function matrixs of $\mathbf{P}_C(t)$ and $\mathbf{P}_0$. However, the viewpoint is not rigorous mathematically that the first mode represents the mean pressure and the following modes represent the fluctuating pressure when $\mathbf{P}_C(t)$ are employed in POD application. When $\mathbf{P}_C(t)$ are employed, POD results of all modes would be distorted by the mean value components, and it's impossible to identify $\mathbf{P}_0$ and $\mathbf{P}_F(t)$ separately. Consequently, characteristics of the fluctuating component, which is always the primary concern in wind pressure field analysis, can only be precisely identified with $\mathbf{P}_0$ excluded in POD.

Keywords: POD; influence mechanism; mean value components; complete fields; fluctuating fields; eigenmodes; eigenvalues

1. Introduction

In wind engineering, it's always a challenge to analyze and capture the characteristics of random fluctuations of the wind pressure fields on bluff bodies which are complicated functions of both time and space, because of the turbulent incoming flow, flow separation, flow reattachment, vortex shedding, wake flow effects, aeroelastic effects and so on (Kareem and Cermak 1984, Chen *et al*. 2004, Li *et al*. 2012). Among many techniques, proper orthogonal decomposition (POD) provides a unique tool to analyze the temporal and spatial characteristics of complex random fields, which is also known as Karhunen-Loève decomposition (KLD) or principal component analysis (PCA). The principles of POD approach and its origin, evolution, and applications in fluid mechanics have been elaborated in detail by many researchers (Lumley 1970, Loève 1978, Tamura

∗Corresponding author, Lecturer, E-mail: brilliantshine@163.com
[a] Professor, E-mail: yaojunge@tongji.edu.cn
[b] Professor, E-mail: zhaolin@tongji.edu.cn

http://www.techno-press.org/?journal=was&subpage=8 ISSN: 1226-6116 (Print), 1598-6225 (Online)

et al. 1999, Liang *et al*. 2002, Chen *et al*. 2004, Taylor and Glauser 2004, Carassale *et al*. 2007, Solari *et al.* 2007, Li *et al*. 2012, Cheng *et al*. 2015) and won't be represented repeatedly.

The most striking feature of POD is that it detects a new coordinate system which can represent the original fluctuating fields and this coordinate system is proved to be the most efficient. In other words, POD technique could represent a random field, which is time-space coupled, as a linear combination of uncoupled space vectors and time series. The space vectors and time series, always referred as to eigenmodes and principal coordinates separately, could be obtained from the random field itself easily. More importantly, these eigenmodes are orthogonal and principal coordinates are uncorrelated. According to this feature, POD method can identify the characteristics hidden in the random fluctuations and thus help us to understand the phenomena better (Holmes 1990, Davenport 1995, Tamura *et al*. 1999, Chen *et al*. 2004, Li *et al*. 2012). This feature is the powerful foundation for the ordinary and extended applications of POD. Owning to the orthogonality of eigenmodes and principal coordinates, POD method provides an efficient method of capturing the dominant components of a complex random field with only very few lower modes, and then the amount of data needed to be stored could be greatly compressed (Bienkiewicz *et al*. 1993, Tamura *et al*. 1999, Chen *et al*. 2004, Chen *et al*. 2011). This is also helpful for the reconstruction and extrapolation of random fields (Solari and Tubino 2002, Chen *et al*. 2004, Hoa 2009, Chen *et al*. 2011). According to the eigenmodes and principal coordinates, physical flow mechanisms (Kareem and Cermak 1984, Baker 2000, Solari *et al*. 2007, Wang *et al*. 2010) and wind-excitation effects (Uematsu *et al*. 2001, Carassale *et al*. 2007, Solari *et al*. 2007, Tubino and Solari 2007, Fiore and Monaco 2009, Hoa 2009) could be further discussed and interpreted.

Although widely used, there is still confusion in the practical application of POD technique: with or without the inclusion of mean value components of wind pressures fields. Some researchers employed POD with the mean value components included (Bienkiewicz *et al*. 1993, Bienkiewicz *et al*. 1995, Davenport 1995, Jeong *et al*. 2000), some without (Holmes 1990, Kikuchi *et al*. 1997, Carassale *et al*. 2007), and some even no explicit descriptions on this question (Letchford and Mehta 1993, Tamura *et al*. 1997, Baker 2000, Chen *et al*. 2011). Evidently, with or without the inclusion of mean value components will give different POD parameters, such as eigenmodes, eigenvalues and principal coordinates, and inevitably distorted interpretations on these POD parameters. The further exploration of the physical flow mechanism would also be confused by these two series of POD parameters. A misconception is that the first mode represents the mean pressure and the following modes represent the fluctuating pressure when the mean value components are included in the POD application (Bienkiewicz *et al*. 1993, Bienkiewicz *et al*. 1995, Tamura *et al*. 1999, Chen *et al*. 2004, Carassale *et al*. 2007). Straightforward seemingly, but this viewpoint is not rigorous according to mathematical explanation, as discussed later.

Actually, whether the mean value components should be included is a critical question for POD application on random fields, such as wind pressure fields. This question has been investigated in several studies (Tamura *et al*. 1999, Chatterjee 2000, Chen *et al*. 2004, Carassale *et al*. 2007). However, most studies just gave superficial analyses through comparative study: merely exhibiting differences between the two series of POD parameters acquired from the random fields with or without the mean value components. These comparative studies failed to reveal the influence mechanism of mean value components on the application of POD, due to the missing of fundamental mathematical analysis. The present work is motivated by this question and this study just focuses on the applications of POD on wind engineering, although it has been applied in many fields including random variable, signal analysis, process identification, and so on (Chen *et al*. 2011).

2. POD method

Let $\mathbf{P}(t)$ be an arbitrary random wind pressure field on a bluff body in three-dimensional space. No matter its mean value is zero or not, it could be written as

$$\mathbf{P}(t) = \{\mathrm{p}(\mathbf{x}_1, t), \mathrm{p}(\mathbf{x}_2, t), \ldots, \mathrm{p}(\mathbf{x}_n, t)\}^T \quad (1)$$

where $\mathbf{x}_i = (x_i, y_i, z_i)$ denotes the position of i-th pressure tap (i=1, 2, …, n) and n is the number of pressure time series used in the ensemble of the pressure field. In an appearance sense, $\mathbf{P}(t)$ could be regarded as a column vector in n-dimension.

According to the POD approach, the eigenmode $\boldsymbol{\phi}$ (i.e., eigenvector) of a random field could be obtained easily from Eq. (2).

$$\mathbf{R\Phi} = \mathbf{\Phi\Lambda} \quad (2)$$

In Eq. (2), $\mathbf{R}$ is the spatial correlation function matrix of $\mathbf{P}(t)$ and $\mathbf{R}$ is a $n\times n$ square matrix. R_{ij}, an element of $\mathbf{R}$ and calculated by Eq. (3), is the zero-time-lag correlation function of wind pressure time series between tap i and j. $\boldsymbol{\phi}_i$ and λ_i denote the i-th eigenvector and i-th eigenvalue of the matrix $\mathbf{R}$ respectively. The eigenvectors and eigenvalues could also be assembled in matrix $\mathbf{\Phi} = \{\boldsymbol{\phi}_1, \boldsymbol{\phi}_2, \ldots, \boldsymbol{\phi}_n\}$ and diagonal matrix $\mathbf{\Lambda} = diag(\lambda_1, \lambda_2, \ldots, \lambda_n)$ respectively. Thus, the principle of POD technique is also regarded as an eigenvalue problem essentially, and Lumley (1967), Loève (1978), Bienkiewicz *et al.* (1993), Tamura *et al*. (1999), Chen *et al*. (2004) have presented more detailed elaboration of the basic definition and principle of POD. In application, eigenvectors are always normalized to have Euclidean length equal to one, i.e., $\boldsymbol{\phi}_i^T\boldsymbol{\phi}_i = 1.0$, and the eigenvalues are ordered decreasingly, for convenience and comparison. This is also adopted in the following study.

$$R_{ij} = \mathrm{E}[\mathrm{p}(\mathbf{x}_i, t)\mathrm{p}(\mathbf{x}_j, t)] \quad (3)$$

According to Eq. (3), the spatial correlation function matrix $\mathbf{R}$ of $\mathbf{P}(t)$ is a real symmetric matrix. Then, its eigenvector matrix $\mathbf{\Phi}$ must exist and is orthogonal, i.e.

$$\boldsymbol{\phi}_i^T\boldsymbol{\phi}_j = \delta_{ij} \qquad \text{or} \qquad \mathbf{\Phi}^T = \mathbf{\Phi}^{-1} \quad (4)$$

and δ_{ij} is Kronecker's delta.

Because of orthogonality, the n eigenvectors, $\boldsymbol{\phi}_1, \boldsymbol{\phi}_2, \ldots, \boldsymbol{\phi}_n$, constitute an independent basis (or a set) for n-dimensional vector space, $\mathbf{V}^n$, and therefore any vector in $\mathbf{V}^n$ could be expressed by linear combination of vectors in this basis. For example, at a specified time point, t_d, the random field $\mathbf{P}(t)$ is regressed into a n-dimensional vector, noted as $\mathbf{P}(t_d)$. Apparently, $\mathbf{P}(t_d)$ belongs to $\mathbf{V}^n$ and could be built by linear combinations of the n eigenvectors as

$$\mathbf{P}(t_d) = \sum_{i=1}^{n} a_i(t_d)\boldsymbol{\phi}_i \qquad \text{or} \qquad \mathbf{P}(t) = \mathbf{\Phi a}(t) \quad (5)$$

where $a_i(t_d)$ is the linear-combination-coefficient of vector $\boldsymbol{\phi}_i$ at time point t_d; $\mathbf{a}(t) = \{a_1(t), a_2(t), \ldots, a_n(t)\}^T$ is the assemblage of $a_i(t)$, in the same form of $\mathbf{P}(t)$. $a_i(t)$ is the time-series-coefficient of mode $\boldsymbol{\phi}_i$, which is also named as the i-th principal coordinate.

Actually, $\mathbf{P}(t)$ could be built by any basis of $\mathbf{V}^n$ mathematically, such as Fourier series, or Legendre polynomials, or Chebyshev polynomials and so on (Chatterjee 2000), with the combination of corresponding time coordinates. However, the POD technique, employing eigenvectors of the spatial correlation function matrix $\mathbf{R}$ of $\mathbf{P}(t)$ as the basis, provides better interpretations on the temporal and spatial underlying features of the random field $\mathbf{P}(t)$.

Since $\mathbf{\Phi}$ is orthogonal and is extracted from $\mathbf{R}$, $a_i(t)$ could be calculated by Eq. (6) and $\mathbf{a}(t)$ could be written as Eq. (7) according to Eqs. (4) and (5). Moreover, $\mathbf{a}(t)$ is also uncorrelated and the mean square of $a_i(t)$ is the i-th eigenvalue of the matrix $\mathbf{R}$ (Eq. (8)).

$$a_i(t) = \boldsymbol{\phi}_i^T \mathbf{P}(t) \tag{6}$$

$$\mathbf{a}(t) = \mathbf{\Phi}^T \mathbf{P}(t) \tag{7}$$

$$E[a_i(t) a_j(t)] = \boldsymbol{\phi}_i^T \mathbf{R} \boldsymbol{\phi}_j = \lambda_i \delta_{ij} \tag{8}$$

The energy of a time series is always defined as its mean square in stochastic engineering. Owning to the uncorrelation of $\mathbf{a}(t)$, the energy or the mean square of wind pressure at a point k could be expressed as

$$E[p(\mathbf{x}_k, t) p(\mathbf{x}_k, t)] = E[\sum_{i=1}^{n} \sum_{j=1}^{n} a_i(t) a_j(t)] \phi_{i,\,k} \phi_{j,\,k} = \sum_{i=1}^{n} \lambda_i \phi_{i,\,k}^2 \tag{9}$$

where $\phi_{i,\,k}$ is the k-th element in eigenvector $\boldsymbol{\phi}_i$.

Furthermore, the total energy of the original field $\mathbf{P}(t)$, S, could be defined as the sum of energy at all pressure points. According to Eq. (8), Eq. (9) and the orthogonality of matrix $\mathbf{R}$, S is equal to the sum of the eigenvalues, which means S is also equal to the sum of the mean squares of the principal coordinates

$$S = \sum_{k=1}^{n} E[p(\mathbf{x}_k, t) p(\mathbf{x}_k, t)] = E[\sum_{i=1}^{n} \sum_{j=1}^{n} a_i(t) a_j(t)] \boldsymbol{\phi}_i^T \boldsymbol{\phi}_j = \sum_{i=1}^{n} \lambda_i = \sum_{i=1}^{n} E[\sum_{i=1}^{n} a_i^2(t)] \tag{10}$$

As a result, the contribution of an eigenmode $\boldsymbol{\phi}_i$ to the original random field could be measured by its eigenvalue λ_i which is an index of the energy stored in eigenmode $\boldsymbol{\phi}_i$, and this is the fundamental advantage to use the eigenvector extracted from $\mathbf{R}$ as the basis. In addition, $a_i(t)$ would not be zero in the whole time-series for a random fluctuating field $\mathbf{P}(t)$, so it can be deduced from Eq. (8) that λ_i would always be positive. This means every eigenmode $\boldsymbol{\phi}_i$ contributes to the whole field more or less and $\mathbf{R}$ is a positive-definite matrix (Hoa 2009).

Similar to the classical mode superposition method in the analysis of structural dynamic responses, reconstruction of the original field $\mathbf{P}(t)$ by limited number of dominant lower eigenmodes would be usually accurate enough in engineering sense because of the decreasing eigenvalue order, as

$$\mathbf{P}(t) \approx \sum_{i=1}^{M} \boldsymbol{\phi}_i a_i(t) \quad (M < n) \tag{11}$$

It means that the POD technique can greatly reduce the amount of data that needs to be stored to re-examine the random wind pressure. The number of eigenmodes that need to be considered can be estimated by the individual proportion w_i and the accumulative proportion w_M, which are defined as (Tamura *et al.* 1999, Chen *et al*. 2011)

$$w_i = \frac{\lambda_i}{S}; w_M = \sum_{i=1}^{M} w_i \tag{12}$$

As stated in the beginning, $\mathbf{P}(t)$ is an arbitrary random wind pressure field, so the procedure of POD technique is valid whether the mean value of $\mathbf{P}(t)$ is zero or not. In practice, the random wind pressure fields obtained directly from wind tunnel model, prototype or simulated by CFD are non-zero-mean inevitably. Thus there would be two conditions for the $\mathbf{P}(t)$ in practical application: $\mathbf{P}_C(t)$, the complete random field containing the mean value component, noted as $\mathbf{P}_0$, and $\mathbf{P}_F(t)$, just the fluctuating field, as written below

$$\mathbf{P}_0(t) = \mathbf{P}_0(\mathbf{x}_i) \tag{13}$$

$$\mathbf{P}_C(t) = \mathbf{P}_0 + \mathbf{P}_F(t) = \mathbf{P}_0(\mathbf{x}_i) + \mathbf{P}_F(\mathbf{x}_i, t) \tag{14}$$

where $\mathbf{P}_C(t)$, $\mathbf{P}_F(t)$, $\mathbf{P}_0$ are all column vector in n-dimension, just like $\mathbf{P}(t)$ in Eq. (1). In addition, the relationship of the total sums of the mean-square field of $\mathbf{P}_C(t)$ and $\mathbf{P}_F(t)$ can be written as

$$\sum_{k=1}^{n} E[\mathbf{P}_C(\mathbf{x}_k, t)\mathbf{P}_C(\mathbf{x}_k, t)] = \sum_{k=1}^{n} E[\mathbf{P}_F(\mathbf{x}_k, t)\mathbf{P}_F(\mathbf{x}_k, t)] + \sum_{k=1}^{n} \mathbf{P}_0^2(\mathbf{x}_k) \tag{15}$$

Another, The time-mean-value of $a_i(t)$ could be wrote as Eq. (16). Obviously, $a_i(t)$ would be zero-mean time series if $\mathbf{P}(t)$ is a zero-mean field as $\mathbf{P}_F(t)$.

$$\mathrm{E}[a_i(t)] = \mathrm{E}[\boldsymbol{\phi}_i^{\mathrm{T}}\mathbf{P}(t)] = \boldsymbol{\phi}_i^{\mathrm{T}}\mathbf{P}_0 \tag{16}$$

Evidently, POD could be applied both on $\mathbf{P}_C(t)$ or $\mathbf{P}_F(t)$, i.e., Eqs. (2)-(10) are valid whether the mean components exist or not. However, the two conditions of data sources will give different correlation function matrix, different POD results, such as eigenmodes, eigenvalues and principal coordinates, and further different interpretation of the random field.

According to Eq. (3), the spatial correlation function matrix $\mathbf{R}$ could be noted as $\mathbf{R}_C$ for $\mathbf{P}_C(t)$ or $\mathbf{R}_F$ for $\mathbf{P}_F(t)$. So, a question or confusion is brought up: Which matrix should be chose for subsequent procedures of POD technique for reasonable and accurate interpretation of the random field $\mathbf{P}_C(t)$, $\mathbf{R}_C$ or $\mathbf{R}_F$? This is a critical question for POD applications, not only in its application in wind engineering.

Meanwhile, some illustrations and applications (Kikuchi *et al*. 1997, Carassale *et al*. 2007) holds the opinion that the matrix used in POD technique for $\mathbf{P}(t)$ should be the spatial covariance matrix, noted as $\mathbf{Q}$, but not the spatial correlation function matrix, $\mathbf{R}$. The element of $\mathbf{Q}$ is written as

$$Q_{ij} = \mathrm{E}[(p(\mathbf{x}_i, t)\text{-}p_0(\mathbf{x}_i, t))(p(\mathbf{x}_j, t)\text{-}p_0(\mathbf{x}_j, t))] \tag{17}$$

Obviously, matrix $\mathbf{Q}_C$ of $\mathbf{P}_C(t)$ is equal to $\mathbf{Q}_F$ of $\mathbf{P}_F(t)$, so matrix $\mathbf{Q}$ can represent both $\mathbf{Q}_C$ and $\mathbf{Q}_F$ and matrix $\mathbf{Q}$ is used in the following discussion. Moreover, $\mathbf{Q}$ is mathematically equal to $\mathbf{R}_F$ of $\mathbf{P}_F(t)$. When $\mathbf{Q}$ but not $\mathbf{R}$ is used in the procedure of POD application for $\mathbf{P}_C(t)$, this situation is essentially that $\mathbf{R}_F$ is used for $\mathbf{P}_F(t)$. Then, the foregoing question could be stated as another but essentially the same question: Which matrix of $\mathbf{P}_C(t)$should be used, $\mathbf{R}$ or $\mathbf{Q}$?

Apparently, the differences between $\mathbf{R}_C$ and $\mathbf{R}_F$ (i.e., $\mathbf{R}$ and $\mathbf{Q}$) stem from the presence of mean value components, as well as the differences between POD results and interpretations of the random field. Therefore, the influence mechanism of mean value components on the application of POD for random fields is the key for the two questions. For POD technique which is a mathematical method essentially, the influence mechanism should be elaborated mathematically as well. Otherwise, the physical interpretation of the POD eigenmodes would also be fictitious (Holmes *et al*. 1997, Hoa 2009).

3. Influence mechanism of mean value components

The influence mechanism of mean value components on the application of POD for random fields should be illustrated through the sources of the POD parameters such as the eigenmodes, eigenvalues and principle coordinates, not only through the differences of these POD parameters.

To illustrate the influence mechanism of mean value components, $\mathbf{P}_0$ is presumed to be static time series or a static determined field, noted as $\mathbf{P}_0(t)=\mathbf{P}_0$, similar but different from $\mathbf{P}_C(t)$ or $\mathbf{P}_F(t)$ which are random fields. Then, a new matrix $\mathbf{R}_0$ is introduced and defined as

$$\mathbf{R}_0 = \mathbf{P}_0\mathbf{P}_0^{\mathrm{T}} \tag{18}$$

and $\mathbf{R}_0$ could be named as the correlation function of the mean value components $\mathbf{P}_0$ or $\mathbf{P}_0(t)$ analogously.

Apparently, the rank of matrix $\mathbf{R}_0$ is one, which means that there is only one non-zero eigenvalue λ_1^0 expressed as

$$\lambda_1^0 = \mathbf{P}_0^{\mathrm{T}}\mathbf{P}_0 = \sum_{k=1}^{n} p_0^2(\mathbf{x}_k) \tag{19}$$

and λ_1^0 is equal to the energy of $\mathbf{P}_0$, noted as S^0, according to Eq. (10). Then, its corresponding normalized eigenvector $\boldsymbol{\phi}_1^0$ is

$$\boldsymbol{\phi}_1^0 = \frac{\mathbf{P}_0}{\sqrt{\mathbf{P}_0^{\mathrm{T}}\mathbf{P}_0}} = \frac{\mathbf{P}_0}{\sqrt{\lambda_1^0}} \tag{20}$$

which is proportional to $\mathbf{P}_0$. Of course there are still other n-1 eigenvectors for $\mathbf{R}_0$ because $\mathbf{R}_0$ is also a real symmetric matrix, just as the spatial correlation function matrix $\mathbf{R}$ in Eq. (3). However, it should be emphasized that the following n-1 eigenvectors $\boldsymbol{\phi}_i^0$ ($i \geq 2$) are not determinate because their eigenvalues are all equal to zeros. In other words, any $\boldsymbol{\phi}_i^0$ ($i \geq 2$) meets the following equation can be eigenvector of $\mathbf{R}_0$.

$$\boldsymbol{\phi}_1^0\boldsymbol{\phi}_i^0 = 0 \quad \textit{and} \quad \boldsymbol{\phi}_i^0\boldsymbol{\phi}_j^0 = \delta_{ij} \quad (i, j \geq 2) \tag{21}$$

On the other hand, because the fist eigenvector $\boldsymbol{\phi}_1^0$ contains the whole energy of $\mathbf{P}_0$, the energy of each following eigenvectors $\boldsymbol{\phi}_i^0$, or λ_i^0 ($i \geq 2$) must be zero. Thus, the following eigenvectors $\boldsymbol{\phi}_i^0$ ($i \geq 2$) has no meaning for $\mathbf{P}_0$, no matter what values they are.

Moreover, if $\mathbf{P}_0$ is regarded as a field, static although, it could also be demonstrated by POD technique. Its POD parameters could also be attracted from $\mathbf{R}_0$ and exhibits some special features. According to Eq. (5), there are n eigenvectors and corresponding principle coordinates for a random field such as $\mathbf{P}_C(t)$ or $\mathbf{P}_F(t)$. For a static field $\mathbf{P}_0$, however, Eq. (5) could be wrote as

$$\mathbf{P}_0 = \sum_{i=1}^{n} \boldsymbol{\phi}_i^0 a_i^0 = \sqrt{\lambda_1^0}\boldsymbol{\phi}_1^0 = a_1^0\boldsymbol{\phi}_1^0 \tag{22}$$

according to Eq. (20). It means that a static field $\mathbf{P}_0$ could be demonstrated by just one eigenvector, $\boldsymbol{\phi}_1^0$. Its corresponding principle coordinate is $a_1^0=\sqrt{\lambda_1^0}$, which could be regarded as a static time series. Also, the following principle coordinate $a_i^0=0$ ($i \geq 2$) because $\lambda_i^0 = 0$.

Furthermore, there is still a relationship among $\mathbf{R}_0$, $\mathbf{R}_C$ and $\mathbf{M}$ (or $\mathbf{R}_F$) that could be expressed as

$$\mathbf{R}_C = \mathbf{M} \text{ (or } \mathbf{R}_F) + \mathbf{R}_0 \tag{23}$$

which could be deduced from Eq. (3), Eqs. (14), (17) and (18) easily. Another, the following equation could be got from Eqs. (10), (15) and (19)

$$S^C = S^F + S^0 (\text{or } \lambda_1^0) \tag{24}$$

where S^C and S^F represent the total energy of $\mathbf{P}_C(t)$ and $\mathbf{P}_F(t)$ respectively.

It has been reported repeatedly that the first eigenvalue got from $\mathbf{R}_C$, i.e., λ_1^C, is almost equal to λ_1^0 and the first eigenmode from $\mathbf{R}_C$, i.e. $\boldsymbol{\phi}_1^C$, is always similar to the distribution of $\mathbf{P}_0$ (Tamura *et al*. 1999, Chen *et al*. 2004). These phenomena are inevitable not only physically but also mathematically. For an ordinary wind pressure field, the complete random field $\mathbf{P}_C(t)$ is always dominated by the static field $\mathbf{P}_0$, even there are extreme fluctuations at certain points. Therefore, most elements in $\mathbf{R}_C$ would be approximately equal to the corresponding elements in $\mathbf{R}_0$, and then, just minute disparity could be detected between the eigenvalues and eigenvectors got from $\mathbf{R}_C$ and $\mathbf{R}_0$, especially for the first mode. So, the gap between λ_1^C and λ_1^0 is minor, as well as the deviation between $\boldsymbol{\phi}_1^C$ and $\boldsymbol{\phi}_1^0$. Given the relationship between $\boldsymbol{\phi}_1^0$ and $\mathbf{P}_0$ (Eq. (20)), almost identical distribution of $\boldsymbol{\phi}_1^C$ and $\mathbf{P}_0$, excluding their amplitudes, would be logically reasoned. Furthermore, other corresponding eigenvalues of $\mathbf{R}_C$ and $\mathbf{R}_0$ would still be close to each other because of the similarity between $\mathbf{R}_C$ and $\mathbf{R}_0$. It means λ_i^C ($i \geq 2$) would be near zero because $\lambda_i^0 = 0$ ($i \geq 2$), and this is also a well-known POD result for $\mathbf{R}_C$. Eventually, it's believed sometimes that the first mode represents the mean pressure and the following modes represent the fluctuating pressure when $\mathbf{P}_C(t)$ and $\mathbf{R}_C$ are employed in the POD application.

However, it should be noted that λ_1^C and λ_1^0 are just close but not equal to each other because of the existence of fluctuating signals in $\mathbf{R}_C$, as well as the distributions of $\mathbf{P}_0$ and $\boldsymbol{\phi}_1^C$. Therefore, the opinion couldn't be accepted that the first eigenmode $\boldsymbol{\phi}_1^C$ and eigenvalue λ_1^C represent the mean component $\mathbf{P}_0$ when $\mathbf{R}_C$ is employed in POD application. Apparently, it could be deduced that the gap between λ_1^C and λ_1^0 would be widen with the increase of the fluctuating signals in $\mathbf{P}_C(t)$}, as shown in Table 3 in the following illustration, as well as the deviation between $\boldsymbol{\phi}_1^C$ and $\boldsymbol{\phi}_1^0$. The deviation between arbitrary two vectors, such as $\boldsymbol{\phi}_1^C$ and $\boldsymbol{\phi}_1^0$, is measured by L_1 norm and L_2 norm of their difference vector $\boldsymbol{\phi}_1^{C\text{-}0}$, also known as Minkowski distance, shown as

$$L_1 = \sum_{j=1}^{n} |\phi_{1,\,j}^{C\text{-}0}|; \quad L_2 = \sqrt{(\sum_{j=1}^{n} |\phi_{1,\,j}^{C\text{-}0}|^2)} \tag{25}$$

in which $\phi_{1,\,j}^{C\text{-}0} = \phi_{1,\,j}^{C} - \phi_{1,\,j}^{0}$ is the *j-th* element in vector $\boldsymbol{\phi}_1^{C\text{-}0}$.

If this is the case, actually as it is, it's also not rigorous to say that the following n-1 eigenmodes $\boldsymbol{\phi}_i^C$ and eigenvalues λ_i^C ($i \geq 2$) represent the fluctuating component $\mathbf{P}_F(t)$. This could be explained in two senses. In mathematics, there must be at least n eigenvectors for the precise reconstruction of the original n-dimension random field $\mathbf{P}(t)$ according to Eq. (5). Therefore, n-1 eigenvectors can't represent a n-dimension random field, such as eigenmode $\boldsymbol{\phi}_i^C$ ($i \geq 2$) for $\mathbf{P}_F(t)$, no matter what linear-combination-coefficients are employed. On the other hand, there is no reasonable interpretation on $\boldsymbol{\phi}_i^C$ ($i \geq 2$) because $\boldsymbol{\phi}_i^C$ would be disturbed inevitably by $\boldsymbol{\phi}_i^0$ ($i \geq 2$) which is meaningless and indeterminate for $\mathbf{P}_0$.

Consequently, POD technique is a wonderful tool to analyze the structures of complex random fields but should be used and interpreted properly. The structure of fluctuating component $\mathbf{P}_F(t)$ is always the primary concern in wind pressure field analysis and it is expected that the mean component $\mathbf{P}_0$ and the fluctuating component $\mathbf{P}_F(t)$ could both be precisely identified from the eigenmodes and eigenvalues. Unfortunately, this is impossible when matrix $\mathbf{R}_C$ is employed in POD application because its eigenmodes and eigenvalues are mixed by the accompanying presences of $\mathbf{P}_0$ and $\mathbf{P}_F(t)$. In other words, it is just correct in mathematics but not practical for application using $\mathbf{R}_C$ in POD because the POD parameters are global reflection of $\mathbf{P}_C(t)$. If $\mathbf{R}_F$ of $\mathbf{P}_F(t)$ (i.e., $\mathbf{M}$ of $\mathbf{P}_C(t)$) is employed, however, the POD results would be pure reflection of the fluctuating component $\mathbf{P}_F(t)$. This mathematical illustration draws a viewpoint that the presence of $\mathbf{R}_0$ in $\mathbf{R}_C$, i.e., the presence of $\mathbf{P}_0$ in $\mathbf{P}_C(t)$, disturbs the eigenmodes and eigenvalues of $\mathbf{R}_C$ which are expected to reflect the structure of $\mathbf{P}_F(t)$. Actually, this viewpoint has been reported by Tamura *et al*. (1999) and Chen *et al*. (2004), but neither illustrated the influence mechanism of mean value components mathematically.

4. POD analysis for several wind pressure fields

4.1 Experimental configuration

As examples demonstrating the influence mechanism of mean value components on the application of POD for random fields, POD analysis for wind pressure fields on a cooling tower and a closed box girder which exhibit quite different cross sections are presented here.

Wind pressure fields were obtained through rigid model tests in wind tunnel. Model dimensions of the cooling tower and the closed box girder section were shown in Fig. 1, as well as the pressure tap layouts. The model scale is 1/200 for the cooling tower and 1/60 for the box girder section. The surface roughness of the cooling tower model was changed to compensate the Reynolds number effect. In order to highlight the influence mechanism of mean value components, wind pressure field of a section but not the whole model surface was employed in POD analysis. Pressure taps of cooling tower locate in two sections and 36 taps distribute uniformly for each section. The length of the closed box girder model is 280 cm and all the 60 pressure taps locate in the middle section. These two model tests were conducted at Tongji University, cooling tower test in wind tunnel TJ-3 and box girder test in wind tunnel TJ-2 separately. The wind pressure was measured simultaneously at all points using the multi-channel simultaneous fluctuating pressure measurement system. The wind environment for cooling tower model was simulated as a suburban terrain with the power-law index of the mean wind speed profile 0.16. Apparently, the wind pressure fields of section A and section B are similar. However, the proportion of mean pressure components of section A is lower than that of section B, because the turbulence intensity decreases with height. For the box girder model, there are two types of wind environment, smooth flow and turbulent flow with turbulence intensity 0.15. Accordingly, two types of wind pressure fields would be obtained from the box girder model and their proportions of mean pressure components are different. Finally, each model has two types of wind pressure fields.

4.2 Distribution of wind pressure coefficient

Figs. 2 and 3 show the mean and the fluctuating wind pressure coefficients (noted as C_P and σ_P) of the two models. They are the temporal mean and the standard deviation of the wind pressure at each point respectively. For the box girder model test, the incoming flow is uniform along the height in wind tunnel TJ-2, so its coefficients are normalized by the mean velocity pressure of incoming flow. For the cooling tower model test, however, the coefficients of the two sections are normalized by the mean velocity pressure of incoming flow at each section elevation, on account of the wind profile. Therefore, the mean coefficients of the two stagnation points both approximate to 1.0.

For the cooling tower model, wind pressure distributions of section A and section B are similar, especially the mean pressure distribution, since they are both circular sections. Both the mean and fluctuating pressure distributions are typical patterns of flow around circular cylinder. Fluctuating coefficients σ_P of section A are higher than those of section B due to the turbulence intensity decreasing with height. For the box girder model, there is no obvious difference between the mean pressure distributions of the two flow conditions, but the fluctuating pressure distributions are quite different. In smooth flow, the fluctuating pressures are quite minor around the whole box girder surface except near tap 10 and tap 57 where wake vortexes shed. In turbulent flow, however, the fluctuating pressures are noticeable around the upstream half surface due to the incoming turbulence.

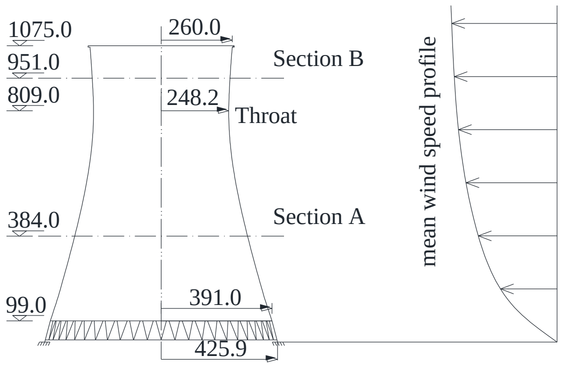

(a) profile of cooling tower model

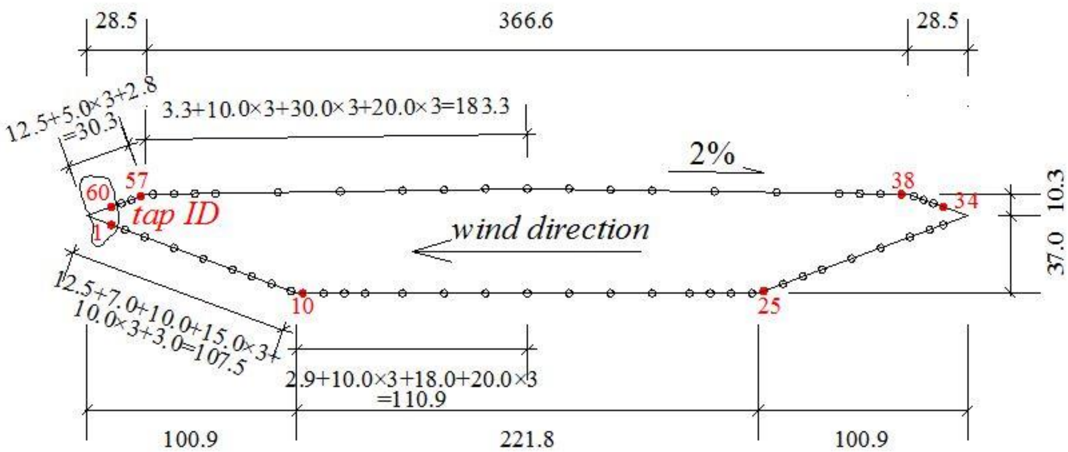

(b) section of closed box girder model

Fig. 1 Pressure measurement model (unit: mm)

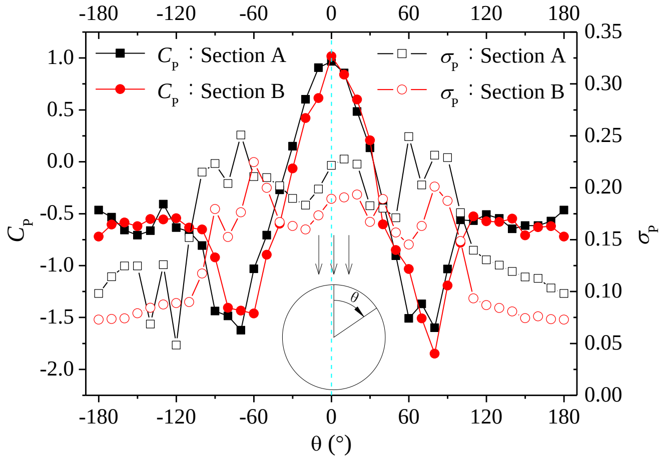

Fig. 2 Wind pressure coefficients of the two sections on the cooling tower model

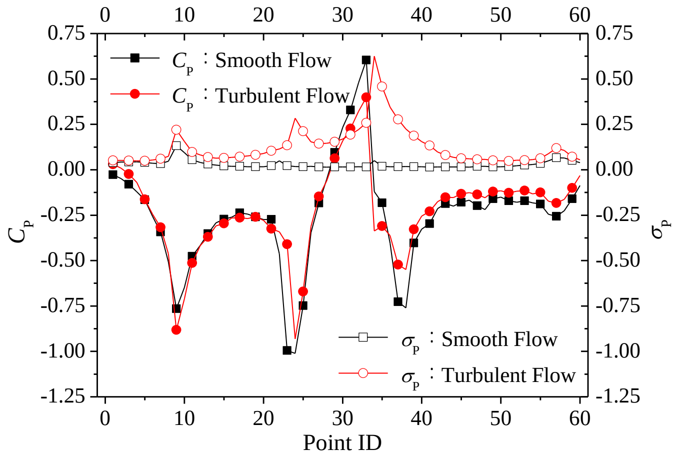

Fig. 3 Wind pressure coefficients of the box girder model in two flows

4.3 POD results analysis

The following presentation will elaborate the influence mechanism in detail according to the POD results got from $\mathbf{R}_C$ and $\mathbf{R}_F$. Tables 1 and 2 give the first five eigenvlaues, and Figs. 4 and 5 describe the first three eigenmodes for the two models. The eigenmodes of the two sections of the cooling tower model are similar because of the similar wind flows around the two sections, so only the eigenmodes of Section B are plotted in Fig. 4. As shown by other authors (Tamura *et al*. 1999, Chen *et al*. 2004), when the mean value is included, as stated in Section 3, λ_1^C and λ_1^0 are close to each other (Column 4 of Table 3), and the first eigenmode $\boldsymbol{\phi}_1^C$ is similar to the mean pressure distribution $\mathbf{P}_0$: eigenmodes $\boldsymbol{\phi}_1^C$ and $\boldsymbol{\phi}_1^0$ are shown almost as one in Figs. 4(a) and 5(a).

Table 1 The first 5 eigenvalues from $\mathbf{R}_C$ and $\mathbf{R}_F$ for cooling tower model

Mode (i)	$\mathbf{R}_C$: mean value included				$\mathbf{R}_F$: mean value excluded			
	Section A (Total energy, S^C: 14.559)		Section B (Total energy, S^C: 20.228)		Section A (Total energy, S^F: 0.510)		Section B (Total energy, S^F: 0.479)	
	Eigenvalue λ_i^C	Proportion (%)	Eigenvalue λ_i^C	Proportion (%)	Eigenvalue λ_i^F	Proportion (%)	Eigenvalue λ_i^F	Proportion (%)
1	14.197 (λ_1^0 = 14.047)	97.51	19.870 (λ_1^0 = 19.745)	98.23	0.161	31.624	0.134	27.963
2	0.078	0.54	0.060	0.29	0.076	14.947	0.055	11.490
3	0.069	0.48	0.048	0.24	0.063	12.373	0.048	10.034
4	0.052	0.36	0.045	0.22	0.049	9.681	0.041	8.496
5	0.022	0.15	0.033	0.17	0.021	4.066	0.033	6.817

Table 2 The first 5 eigenvalues from $\mathbf{R}_C$ and $\mathbf{R}_F$ for box girder model

Mode (i)	$\mathbf{R}_C$: mean value included				$\mathbf{R}_F$: mean value excluded			
	Smooth flow (Total energy, S^C: 8.728)		Turbulent flow (Total energy, S^C: 8.093)		Smooth flow (Total energy, S^F: 0.080)		Turbulent flow (Total energy, S^F: 1.616)	
	Eigenvalue λ_i^C	Proportion (%)	Eigenvalue λ_i^C	Proportion (%)	Eigenvalue λ_i^C	Proportion (%)	Eigenvalue λ_i^C	Proportion (%)
1	8.654 (λ_1^0 = 8.647)	99.16	6.752 (λ_1^0 = 6.476)	83.42	0.050	62.36	1.106	68.41
2	0.047	0.53	1.021	12.61	0.006	7.64	0.201	12.42
3	0.004	0.04	0.085	1.06	0.003	4.38	0.084	5.19
4	0.003	0.04	0.069	0.85	0.003	3.21	0.069	4.27
5	0.003	0.03	0.050	0.62	0.002	3.00	0.044	2.74

Table 3 Results analysis of the first mode from $\mathbf{R}_C$

Model condition	S^F/S^C (%)	λ_1^C/S^C (%)	$1-\lambda_1^0/\lambda_1^C$ (%)	L_1 in Eq. (25)	$1-(\lambda_1^0+\lambda_1^F)/\lambda_1^C$ (%)
Box girder model in smooth flow	0.91	99.16	0.09	0.007	-0.49
Section B of cooling tower model	2.37	98.23	0.63	0.008	-0.05*
Section A of cooling tower model	3.05	97.51	1.05	0.012	-0.08*
Box girder model in Turbulent flow	19.97	83.42	4.08	0.236	-12.29

Note: * in column 6 indicates $\boldsymbol{\phi}_1^F$ and $\boldsymbol{\phi}_1^C$ are similar.

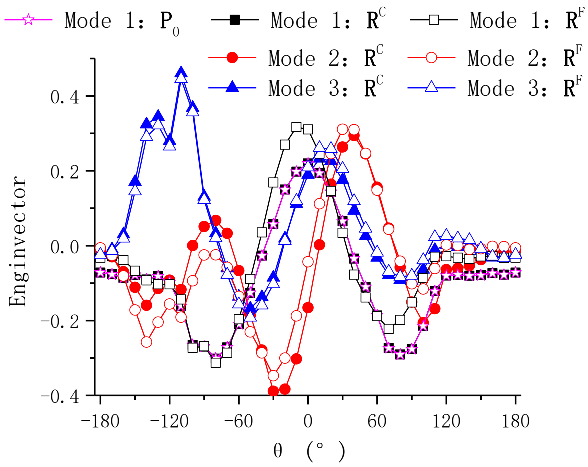

Fig. 4 Mode distributions for section B of cooling tower model

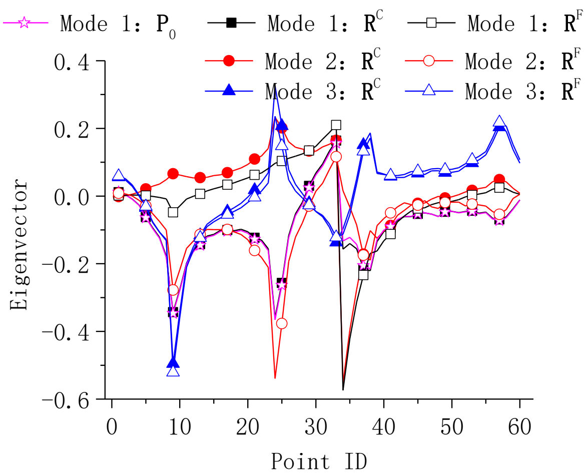

Fig. 5 Mode distributions for box girder model in turbulent flow

Moreover, the first eigenvalue λ_1^C is outstanding extremely and almost equal to the total mean square of the complete random field S^C: the energy proportion of the first eigenmode, i.e., λ_1^C/S^C, are higher than 97% because of the vastly dominated mean value components in the complete pressure fields, except the box girder model in turbulent flow, 83.42%, which is attributable to the more fluctuating pressure than other three situations, as shown in the first column of Table 3. Actually, λ_1^C/S^C would decreases with the increase of the fluctuating component in the complete pressure signal, i.e., S^F/S^C (Table 3). Also, the gap between λ_1^0 and λ_1^C, noted as 1-λ_1^0/λ_1^C in Table 3, is widen with the increase of S^F/S^C, as stated in Section 3, as well as the gap between $\boldsymbol{\phi}_1^C$ and $\boldsymbol{\phi}_1^0$ measured by L_1 in Eq. (25). Thus it can be seen that the higher mean value component in $\mathbf{P}_C(t)$, the greater of its domination on the first mode. Despite the fist mode result dominated by the mean value component, other mode results would also be influenced by the mean value component if it is included in POD application. So the following mode results from $\mathbf{R}_C$ and $\mathbf{R}_F$ are still different, including eigenvalues and eigenmodes, as shown in Tables 1 and 2, Figs. 4 and 5.

A confounding phenomenon is a desired entry point. It can be seen in Figs. 4 and 5 that there are some eigenmodes got from $\mathbf{R}_F$ are close to those got from $\mathbf{R}_C$. For example, $\boldsymbol{\phi}_1^C$ to $\boldsymbol{\phi}_3^C$ in Fig. 4(a) and $\boldsymbol{\phi}_1^F$ to $\boldsymbol{\phi}_3^F$ in Fig. 4(b), $\boldsymbol{\phi}_2^C$ in Fig. 5(a) and $\boldsymbol{\phi}_1^F$ in Fig. 5(b), $\boldsymbol{\phi}_3^C$ in Fig. 5(a) and $\boldsymbol{\phi}_3^F$ in Fig. 5(b). The similarity lies just in mathematical result, but the influence mechanism of mean value components could be draught, as well as some physical interpretation of the wind pressure characteristics.

The similarity of $\boldsymbol{\phi}_1^F$ and $\boldsymbol{\phi}_1^C$, which is valid for the two sections of cooling tower model but not valid for the box girder model, indicates $\boldsymbol{\phi}_1^F$ is similar to $\boldsymbol{\phi}_1^0$ because $\boldsymbol{\phi}_1^C$ is always close to $\boldsymbol{\phi}_1^0$. Therefore, in the POD analysis of $\mathbf{P}_C(t)$, $\boldsymbol{\phi}_1^C$ actually represents the mean pressure distribution $\mathbf{P}_0$ and the dominant spatial component of $\mathbf{P}_F(t)$} meanwhile, i.e., both $\boldsymbol{\phi}_1^0$ and $\boldsymbol{\phi}_1^F$. Therefore, if this is the case, the opinion would be untenable that the first mode represents the mean pressure and the following modes represent the fluctuating pressure when $\mathbf{R}_C$ are used in POD application. This can also be proved by the eigenvalues of λ_1^C and the sum of λ_1^0 and λ_1^F. When $\boldsymbol{\phi}_1^F$ and $\boldsymbol{\phi}_1^C$ are close, the gap between λ_1^C and the sum of λ_1^0 and λ_1^F would be even smaller than the gap between λ_1^C and λ_1^0, as shown in column 4 and column 6 in Table 3 for the cooling tower model. Additionally, the first principle coordinates got from $\mathbf{R}_C$ and $\mathbf{R}_F$ almost appear as one in Fig. 6. Actually, the similarity of $\boldsymbol{\phi}_1^C$ and $\boldsymbol{\phi}_1^F$, is just a coincidence mathematically but reveal a special feature of the random field physically: the similarity of $\boldsymbol{\phi}_1^F$ and $\boldsymbol{\phi}_1^0$.

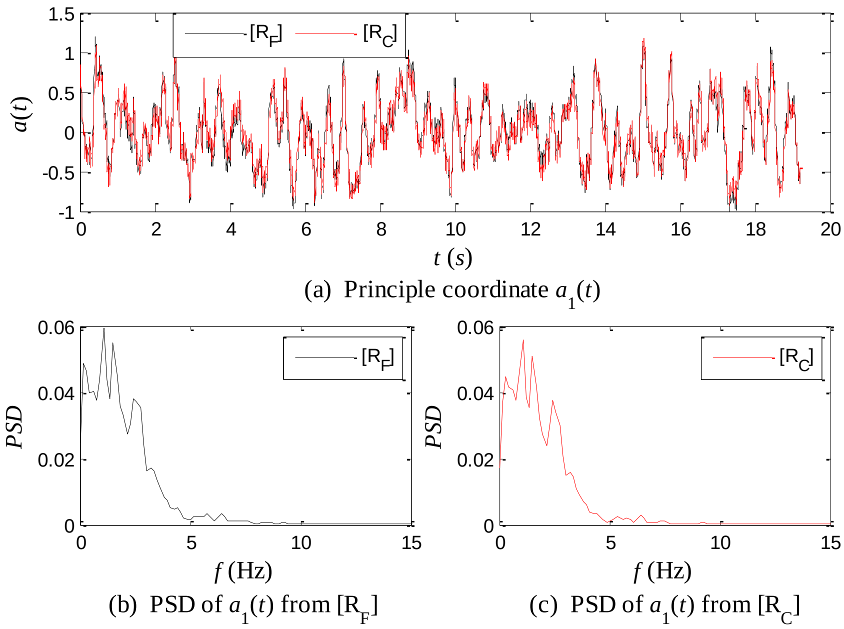

Fig. 6 Principle coordinate $a_1(t)$ and its power spectral density got from $\mathbf{R}_C$ and $\mathbf{R}_F$ for section A of cooling tower model (the mean component of $a_1(t)$ from $\mathbf{R}_C$ is excluded)

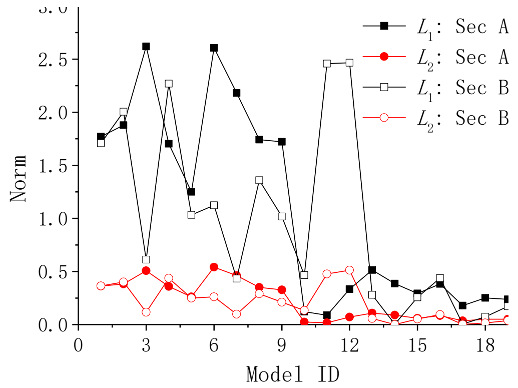

Fig. 7 Vector norms of the difference of corresponding modes from $\mathbf{R}_C$ and $\mathbf{R}_F$ of cooling tower model

In an extreme condition, when $\boldsymbol{\phi}_1^F$ is equal to $\boldsymbol{\phi}_1^0$, Eq. (26) can be deduced from Eq. (2), Eq. (7), Eqs. (21)-(23). Of course λ_i^0 and a_i^0 are all zero for $i \geq 2$ as stated in Section 3. It can be further deduced that the POD result of $\mathbf{R}_F$ and $\mathbf{R}_0$ can be superposed for $\mathbf{R}_C$ only if $\boldsymbol{\phi}_1^F$ is equal to $\boldsymbol{\phi}_1^0$.

$$\phi_i^F = \phi_i^0 = \phi_i^C \quad and \quad \lambda_i^C = \lambda_i^0 + \lambda_i^F \quad and \quad a_i^C(t) = a_i^0(t) + a_i^F(t) \tag{26}$$

In fact, the equality of $\boldsymbol{\phi}_1^F$ and $\boldsymbol{\phi}_1^0$ is just a hypothesis and not practical for random fields, but this extreme condition can explain why λ_1^C and the sum of λ_1^0 and λ_1^F are closer than λ_1^C and λ_1^0 when $\boldsymbol{\phi}_1^F$ is similar to $\boldsymbol{\phi}_1^0$.

Furthermore, due to the similarity of $\boldsymbol{\phi}_1^F$ and $\boldsymbol{\phi}_1^C$ for the two sections of cooling tower model, most of their following eigenmodes and eigenvalues are close to each other correspondingly as well, and this can also be explained by Eq. (26). The similarity between eigenmodes can be measured by L_1 and L_2 norms of vector $\boldsymbol{\phi}_i^{C\text{-}F}$, which is the difference vector of $\boldsymbol{\phi}_i^C$ and $\boldsymbol{\phi}_i^F$ and could be defined by Eq. (25) analogously. The two norms are shown in Fig. 7 and the lower norm value implies the greater similarity between $\boldsymbol{\phi}_i^C$ and $\boldsymbol{\phi}_i^F$. It can be seen from Fig. 4 that the top three eigenmodes are similar, and their norm values are higher than most other following modes. Therefore, it can be deduced that almost all $\boldsymbol{\phi}_i^C$ and $\boldsymbol{\phi}_i^F$ resemble to each other correspondingly. The similarity between the following eigenmodes can also be confirmed by the eigenvalues listed in Table 1: λ_i^C and λ_i^F are close to each other for i=2~5. The following principle coordinates got from $\mathbf{R}_C$ and $\mathbf{R}_F$ are close as well.

Finally, when $\boldsymbol{\phi}_1^F$ and $\boldsymbol{\phi}_1^C$ are similar, it means the dominant spatial component of $\mathbf{P}_F(t)$ resembles the mean pressure distribution $\mathbf{P}_0$, and the first eigenmode of $\mathbf{P}_C(t)$ would represent both $\boldsymbol{\phi}_1^0$ and $\boldsymbol{\phi}_1^F$ approximately. In other words, the POD results of $\mathbf{P}_C(t)$ could be deemed as the superposition of those of $\mathbf{P}_0$ and $\mathbf{P}_F(t)$ for easer interpretation.

For the box girder model, their $\boldsymbol{\phi}_1^F$ and $\boldsymbol{\phi}_1^C$ ($\boldsymbol{\phi}_1^0$) are quite different from each other. In this case, the first eigenmode of $\mathbf{P}_C(t)$ just mainly represent $\mathbf{P}_0$ as usual but not the superposition of $\boldsymbol{\phi}_1^0$ and $\boldsymbol{\phi}_1^F$, and its following eigenmodes mainly represent $\mathbf{P}_F(t)$. Accidentally, there would be some similar eigenmodes between $\boldsymbol{\phi}_i^C$ ($2 \leq i \leq n$) and $\boldsymbol{\phi}_i^F$ ($1 \leq i \leq n$), such as $\boldsymbol{\phi}_2^C$ and $\boldsymbol{\phi}_1^F$, $\boldsymbol{\phi}_3^C$ and $\boldsymbol{\phi}_3^F$ for the box girder model in turbulent flow (Fig. 5), and their corresponding eigenvalue are close as well (Table 2). However, the similarity between the following modes has no further sense.

5. Conclusions

The influence mechanism of mean value components on POD applications for random fields with or without the mean value components included are illustrated mathematically, based on the principles of POD method and matrix analysis. The introduction of a new matrix $\mathbf{R}_0$ and its POD results are the critical philosophy in the illustration, which is defined as the correlation function of the mean value component $\mathbf{P}_0$. Then, POD analyses for several different wind pressure fields, with or without the mean value components, were presented comparatively as convincing examples.

The following well-known POD result characteristics for $\mathbf{R}_C$ are inevitable on account of the mathematical illustration, such as the similarity between $\boldsymbol{\phi}_1^C$ and $\mathbf{P}_0$ (i.e., $\boldsymbol{\phi}_1^0$), close values of λ_1^C and the energy of $\mathbf{P}_0$ (i.e., λ_1^0), nearly zero λ_i^C ($i \geq 2$). Firstly, for matrix $\mathbf{R}_0$, there is only one non-zero eigenvalue λ_1^0 which is equal to the energy of $\mathbf{P}_0$ and its eigenmode $\boldsymbol{\phi}_1^0$ is proportional to $\mathbf{P}_0$. Secondly, most elements in $\mathbf{R}_C$ would be approximately equal to the corresponding elements in $\mathbf{R}_0$, because $\mathbf{P}_C(t)$ is always dominated by $\mathbf{P}_0$ for an ordinary wind pressure field. Therefore, just minute disparity could be detected between the eigenvalues and eigenvectors got from $\mathbf{R}_C$ and $\mathbf{R}_0$, especially for the first mode. Nevertheless, there is no reasonable interpretation on $\boldsymbol{\phi}_i^C$ ($i \geq 2$) because $\boldsymbol{\phi}_i^C$ would be disturbed inevitably by $\boldsymbol{\phi}_i^0$ ($i \geq 2$) which is meaningless and indeterminate for $\mathbf{P}_0$.

Due to the well-known POD result characteristics, a misconception maybe accepted carelessly that the first mode represents the mean pressure and the following modes represent the fluctuating pressure when $\mathbf{P}_C(t)$ are employed in the POD application. However, this viewpoint is not rigorous according to the mathematical explanation. The distributions of $\boldsymbol{\phi}_1^C$ and $\mathbf{P}_0$ are just close to each other, as well as the values of λ_1^C and the energy of $\mathbf{P}_0$. The similarity of POD results, either $\boldsymbol{\phi}_1^C$ and $\boldsymbol{\phi}_1^0$ or λ_1^C and λ_1^0, stems from the similarity of $\mathbf{R}_C$ and $\mathbf{R}_0$. If $\mathbf{P}_F(t)$ increases in $\mathbf{P}_C(t)$, the similarity of $\mathbf{R}_C$ and $\mathbf{R}_0$ would decrease, as well as the POD results.

In a special condition, when $\boldsymbol{\phi}_1^F$ and $\boldsymbol{\phi}_1^0$ resemble to each other, $\boldsymbol{\phi}_1^C$ would also resemble to them; λ_1^C would be closer to the sum of λ_1^0 and λ_1^F than λ_1^0 alone. In other words, the POD results of $\mathbf{P}_C(t)$ could be deemed as the approximate superposition of those of $\mathbf{P}_0$ and $\mathbf{P}_F(t)$ for easer interpretation. In this condition, it would be more absurd to say the first mode represents the mean pressure and the following modes represent the fluctuating pressure if $\mathbf{P}_C(t)$ are employed in the POD application.

As a mathematical technique, POD could be applied on $\mathbf{P}_C(t)$ or $\mathbf{P}_F(t)$ no matter $\mathbf{P}_0$ exists or not. When $\mathbf{R}_C$ are employed in POD, the POD results are global reflection of $\mathbf{P}_C(t)$, and it's impossible to precisely identify $\mathbf{P}_0$ and $\mathbf{P}_F(t)$ separately. Consequently, characteristics of the fluctuating component $\mathbf{P}_F(t)$, which is always the primary concern in wind pressure field analysis, can only be precisely identified when $\mathbf{R}_F$ (i.e., $\mathbf{M}$ of $\mathbf{P}_C(t)$) is employed in POD.

Acknowledgements

The authors would like to gratefully acknowledge the supports of the National Science Foundation of China (51508523, 2009ZX06004-010-HYJY-21).

References

Baker, C.J. (2000), "Aspects of the use of proper orthogonal decomposition of surface pressure fields", *Wind Struct.*, **3**(2), 97-115.
Bienkiewicz, B., Ham, H.J. and Sun, Y. (1993), "Proper orthogonal decomposition of roof pressure", *J. Wind Eng. Ind. Aerod.*, **50**(1-3), 193-202.
Bienkiewicz, B., Tamura, Y., Ham, H.J., Ueda, H. and Hibi, K. (1995), "Proper orthogonal decomposition and reconstruction of multi-channel roof pressure", *J. Wind Eng. Ind. Aerod.*, **54-55**, 369-381.
Carassale, L., Solari, G. and Tubino, F. (2007), "Proper orthogonal decomposition in wind engineering. Part 2: Theoretical aspects and some applications", *Wind Struct.*, **10**(2), 177-208.
Chatterjee, A. (2000), "An introduction to proper orthogonal decomposition", *Current Sci.*, **78**(7), 808-817.
Chen, M.Y., Zhang, J.S. and Zhou, G.G. (2011), "Application of proper orthogonal decomposition technique in wind engineering of structures", *Adv. Mater. Res.*, **250-253**, 2678-2681.
Chen, Y., Kopp, G.A. and Surry, D. (2004), "Spatial extrapolation of pressure time series on low buildings using proper orthogonal decomposition", *Wind Struct.*, **7**(6), 373-392.
Cheng, L., Lam, K.M. and Wong, S.Y. (2015), "POD analysis of crosswind forces on a tall building with square and H-shaped cross sections", *Wind Struct.*, **21**(1), 63-84.
Davenport, A.G. (1995), "How can we simplify and generalize wind loads?", *J. Wind Eng. Ind. Aerod.*, **54-55**, 657-669.
Fiore, A. and Monaco, P. (2009), "POD-based representation of the alongwind equivalent static force for long-span bridges", *Wind Struct.*, **12**(3), 239-257.
Hoa, L.T. (2009), "Proper orthogonal decomposition and recent advanced topics in wind engineering", *VNU J. Science, Mathematics - Physics*, **25**(1), 21-38.
Holmes, J.D. (1990), "Analysis and synthesis of pressure fluctuations on bluff bodies using eigenvectors", *J. Wind Eng. Ind. Aerod.*, **33**(1-2), 219-230.
Holmes, J.D., Sankaran, R., Kwok, K.C.S. and Syme, M.J. (1997), "Eigenvector modes of fluctuating pressures on low-rise building models", *J. Wind Eng. Ind. Aerod.*, **69-71**, 697-707.
Jeong, S.H., Bienkiewicz B. and Ham, H.J. (2000), "Proper orthogonal decomposition of building wind pressure specified at non-uniformly distributed pressure taps", *J. Wind Eng. Ind. Aerod.*, **87**(1), 1-14.
Kareem, A. and Cermak, J.E. (1984), "Pressure fluctuations on a square building model in boundary-layer flows", *J. Wind Eng. Ind. Aerod.*, **16**(1), 1753-1763.
Kikuchi, H., Tamura, Y., Ueda, H. and Hibi, K. (1997), "Dynamic wind pressures acting on a tall building model - proper orthogonal decomposition", *J. Wind Eng. Ind. Aerod.*, **69-71**, 631-646.
Letchford, C.W. and Mehta, K.C. (1993), "The distribution and correlation of fluctuating pressures on the Texas Tech Building", *J. Wind Eng. Ind. Aerod.*, **50**(1-3), 225-234.
Li, F.H., Gu, M., Ni, Z.H. and Shen S.Z. (2012), "Wind pressures on structures by proper orthogonal decomposition", *J. Civil Eng. Architecture*, **6**(2), 238-243.
Liang, Y.C., Lee, H.P., Lim, S.P., Lin, W.Z., Lee, K.H. and Wu, C.G. (2002), "Proper orthogonal decomposition and its applications-Part I: Theory", *J. Sound Vib.*, **252**(3), 527-544.
Loève, M. (1978), Probability Theory II (4th Edn.), New York, Springer-Verlag.
Lumley, J.L. (1970), Stochastic Tools in Turbulence, New York, Academic Press.
Ricciardelli, F., de Grenet, E.T. and Solari G. (2002), "Analysis of the wind loading of a bridge deck box section using proper orthogonal decomposition", *Int. J. Fluid Mech. Res.*, **29**(3-4), 312-322.
Solari, G. and Tubino, F. (2002), "A turbulence model based on principal components", *Probabilist. Eng. Mech.*, **17**(4), 327-335.
Solari, G., Carassale, L. and Tubino, F. (2007), "Proper orthogonal decomposition in wind engineering. Part 1: A state-of-the-art and some prospects", *Wind Struct.*, **10**(2), 153-176.
Tamura, Y., Suganuma, S., Kikuchi, H. and Hibi, K. (1999), "Proper orthogonal decomposition of random wind pressure field", *J. Fluid. Struct.*, **13**(7-8), 1069-1095.
Tamura, Y., Ueda, H., Kikuchi, H., Hibi, K., Suganuma, S. and Bienkiewicz, B. (1997), "Proper orthogonal decomposition study of approach wind-building pressure correlation", *J. Wind Eng. Industrial*

Aerodynamics, **72**(1-3): 421-431.
Taylor, J.A. and Glauser, M.N. (2004), "Towards practical flow sensing and control via POD and LSE based low-dimensional tools", *J. Fluids Eng. T. - ASME*, **126**(3), 337-345.
Tubino, F. and Solari, G. (2007), "Gust buffeting of long span bridges: Double Modal Transformation and effective turbulence", *Eng. Struct.*, **29**(8), 1689-1707.
Uematsu, Y., Kuribara, O., Yamada, M., Sasaki, A. and Hongo, T. (2001), "Wind-induced dynamic behavior and its load estimation of a single-layer latticed dome with a long span", *J. Wind Eng. Ind. Aerod.*, **89**(14-15), 1671-1687.
Wang, L., Wang, Y., Li, Z.Q. and Zhang, Y. (2010), "Estimation of the vortex shedding frequency of a 2-D building using correlation and the POD methods", *J. Wind Eng. Ind. Aerod.*, **98**(12), 895-902.

CC